2

Acousto-Optically Q-Switched CO_2 Laser

Jijiang Xie and Qikun Pan
Changchun Institute of Optics, Fine Mechanics and Physics, Chinese Academy of Sciences
State Key Laboratory of Laser Interaction with Matter
China

1. Introduction

The compacted CO_2 laser with narrow pulse width and high repetition frequency has great potential applications, such as echo-splitting radar (Kariminezhad et al., 2010; Carr et al. 1994), laser processing (Hong et al., 2002), environmental monitor (Zelinger et al., 2009), laser medical instrument (Hedayatollahnajafi et al., 2009), laser-matter interaction (Chang & Jiang, 2009), etc. In fact, currently compacted CO_2 laser is usually implemented with pulsed output by electro-optically Q-switch (Tian et al., 2001) and mechanical Q-switch (Kovacs et al., 1966), and the related theories and technologies are relative maturity. But the method of electro-optically Q-switch often needs high voltage, more between different molecules in the laser gain medium; third, according to various factors (optical loss in cavity, transmittance of output mirror and so on) influencing the output performances of laser, the theoretical and experimental researches are implemented to optimize the design of compacted CO_2 laser; forth, the tunable design with grating has been finished and the spectrum lines are measured in the experiment; fifth, the experiments that laser irradiated HgCdTe detectors are implemented with the acousto-optically Q-switched CO_2 laser.
Both the theory and experiments show that acousto-optically Q-switch is an effective technical method to realize the laser output with narrow pulse width and high repetition frequency. The compacted size acousto-optically Q-switched CO_2 laser which has been optimally-designed realizes 100 kHz repetitive frequency. The full band of wavelength tuning between 9.2μm and 10.8μm is obtained by grating selection one by one. With the further development of acousto-optically modulator, the performance will be greatly improved which will provide an effective method to realize high repetition frequency pulse for CO_2 laser.

2. Acousto-optically Q-switched CO_2 laser

2.1 Acousto-optically Q-switch

Acousto-optically Q-switch is a key component of CO_2 laser to realize pulse output. The acousto-optically Q-switch is composed by driving unit and acousto-optically modulator which is inserted in the cavity. The principle of acousto-optically modulator is the refraction index of crystal changed by using ultrasonic wave as it is transmitting through crystal. The crystal with periodic variation of the refraction index is as the same as a phase grating. When optical beam propagates this crystal, it will create a diffractive wave to realize the

optical beam deflection i.e. Bragg diffraction, as Fig. 1(a). The working principle of acousto-optically Q-switch is shown as Fig. 1(b). The ultrasonic wave is generated by radio frequency (RF) signal with several tens MHz through acousto-optically transducer. Therefore, whether the optical beam is in the condition of deflection or not is totally determined by RF signal controlled by transistor-transistor logic level. When the transistor-transistor logic level is located in high level, the ultrasonic equivalent phase grating will make the optical beam deflection. The deflective angle can completely make the optical beam escape the resonator, which the resonator is in the state of high loss and low Q value. The resonator cannot form the oscillation which means the Q-switch "close" laser. When the transistor-transistor logic level is laid on low level, the RF signal suddenly stops and the ultrasonic field in the Q-switched crystal disappears. This means the switch "open" and the resonator resumes the high Q value with oscillated optical beam output. Accordingly, Q value alternates one time that will generate a Q-switched pulse output from laser. At the same time, if the transistor-transistor logic level is carried out an encoded control, it will realize the encoded pulses output of laser.

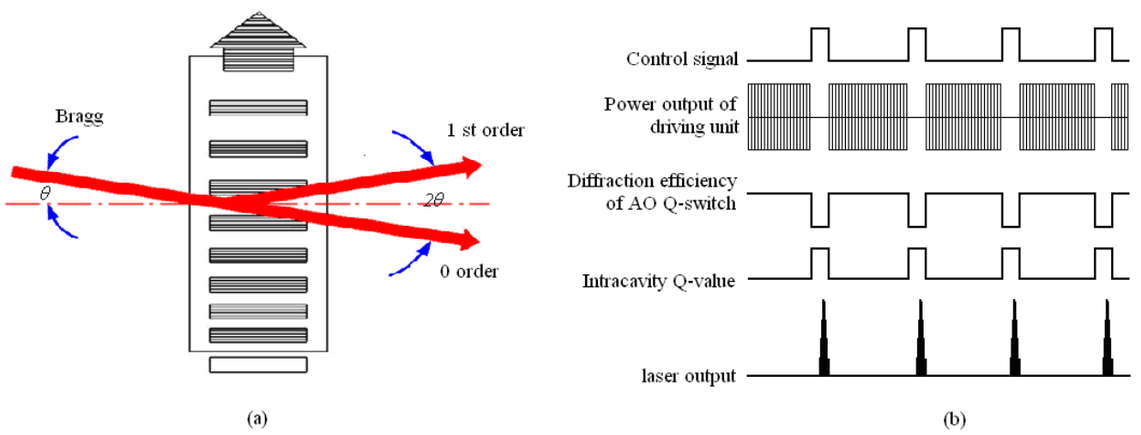

Fig. 1. The scheme of Q-switch

2.2 Basic structure of CO_2 laser

The principle scheme of CO_2 laser is shown in Fig. 2.The laser resonator adopts half external cavity structure with direct current discharge gain area. The diffraction efficiency of acousto-optically modulator is higher when the incident laser is linearly polarized light. Under this condition, the performance of acousto-optically Q-switch is better. This structure is propitious to realize linearly polarized laser output and reduce optical loss, which is helpful for laser output with Q-switch.

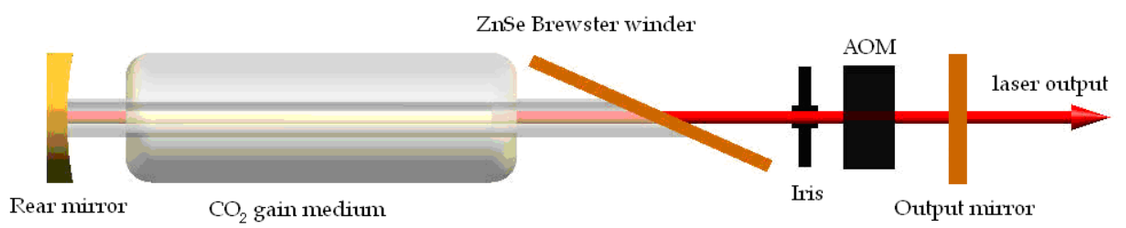

Fig. 2. Schematic diagram of acousto-optically Q-switch CO_2 laser

The discharge tube is made by glass with water cooled pipe. The rear mirror is a spherical mirror coated with gold, and the Brewster window is made by ZnSe material. The working gas is made up of Xe, CO_2, N_2, He. The acousto-optically Q-switch is inserted between the output mirror and the Brewster window. An iris with adjustable aperture size is inserted in the resonator.

3. Dynamical analysis of acousto-optically Q-switched CO_2 laser

3.1 The six-temperature model for acousto-optically Q-switched CO_2 laser

Based on the theory of five-temperature model of the dynamics for CO_2 laser (Manes & Seguin, 1972), the dissociating influence of CO_2 to CO molecules on laser output is concerned. Thus the equivalent vibrational temperature of the CO molecules is taken as a variable quantity of the differential equations for this model. Then the differential equations include six variable quantity of temperature.

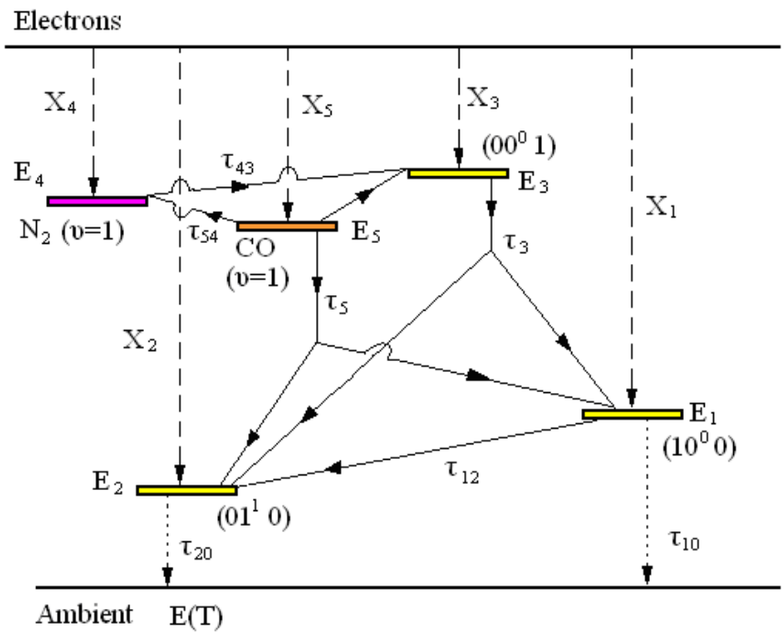

Fig. 3. Schematic energy-level diagram for N_2-CO_2-CO system

In figure 3, we present a schematic diagram of the set of processes of electron collision excitation for CO_2, N_2, and CO molecules, all kinds of energy transfer among molecules, and excited emission and spontaneous emission. The distribution of vibrational energy in different vibrational modes can be described by the following equations (Smith & Thomson, 1978):

$$\frac{dE_1}{dt} = n_e(t) fn_{co_2} X_1 h\nu_1 - \frac{E_1 - E_1(T)}{\tau_{10}(T)} - \frac{E_1 - E_1(T_2)}{\tau_{12}(T_2)} + \\ + \frac{h\nu_1}{h\nu_3} \frac{E_3 - E_3(T, T_1, T_2)}{\tau_3(T, T_1, T_2)} + \frac{h\nu_1}{h\nu_5} \frac{E_5 - E_5(T, T_1, T_2)}{\tau_5(T, T_1, T_2)} + h\nu_1 \Delta NWI_{v_0} \tag{1}$$

$$\frac{dE_2}{dt} = n_e(t) f n_{co_2} X_2 h\nu_2 + \frac{h\nu_2}{h\nu_3}\frac{E_3 - E_3(T, T_1, T_2)}{\tau_3(T, T_1, T_2)} + \\ + \frac{E_1 - E_1(T_2)}{\tau_{12}(T_2)} - \frac{E_2 - E_2(T)}{\tau_{20}(T)} + \frac{h\nu_2}{h\nu_5}\frac{E_5 - E_5(T, T_1, T_2)}{\tau_5(T, T_1, T_2)} \quad (2)$$

$$\frac{dE_3}{dt} = n_e(t) f n_{co_2} X_3 h\nu_3 + \frac{E_4 - E_4(T_3)}{\tau_{43}(T)} - \frac{E_3 - E_3(T, T_1, T_2)}{\tau_3(T, T_1, T_2)} + \frac{h\nu_3}{h\nu_5}\frac{E_5 - E_5(T, T_3)}{\tau_{53}(T, T_3)} - h\nu_3 \Delta NWI_{v_0} \quad (3)$$

$$\frac{dE_4}{dt} = n_e(t) f n_{N_2} X_4 h\nu_4 - \frac{E_4 - E_4(T_3)}{\tau_{43}(T)} + \frac{h\nu_4}{h\nu_5}\frac{E_5 - E_5(T, T_4)}{\tau_{54}(T, T_4)} \quad (4)$$

$$\frac{dE_5}{dt} = n_e(t)(1 - f) n_{co_2} X_5 h\nu_5 - \frac{E_5 - E_5(T, T_3)}{\tau_{53}(T, T_3)} - \frac{E_5 - E_5(T, T_1, T_2)}{\tau_5(T, T_1, T_2)} - \frac{E_5 - E_5(T, T_4)}{\tau_{54}(T, T_4)} \quad (5)$$

Where n_{CO_2} and n_{N_2} are, respectively, the number density of CO_2 and N_2 molecules per unit volume and $n_e(t)$ is the number density of electrons per unit volume. T_1 is the equivalent vibrational temperature of the CO_2 symmetrical stretching mode. T_2 is the equivalent vibrational temperature of the CO_2 bending mode. T_3 is the equivalent vibrational temperature of the CO_2 asymmetric mode. T_4 is the equivalent vibrational temperature of the N_2 molecules. T_5 is the equivalent vibrational temperature of the CO molecules. Eqs. (1)-(3) describe the variation in the stored energy in unit volume (erg/cm^3) as a function of time in CO_2 symmetrical, bending, and asymmetrical modes respectively. Eq. (4) expresses the time evolution of the stored energy density in unit volume for N_2 molecules. Eq. (5) expresses the time evolution of the stored energy density in unit volume for CO molecules, which are dissociated by CO_2 molecules. f is the non-dissociated fraction of CO_2 molecules. For simplicity f is considered as a constant in this paper (in general f is a function of time, electrical field intensity and electron number density).

By taking the sum of Eqs. (1)-(5) in the steady state, the following equation which describes the time evolution of the stored energy density in gas mixture CO_2-N_2-He-CO will be obtained:

$$\frac{dE_K}{dt} = \frac{E_1 - E_1(T)}{\tau_{10}(T)} + \frac{E_2 - E_2(T)}{\tau_{20}} + (1 - \frac{h\nu_1}{h\nu_3} - \frac{h\nu_2}{h\nu_3})\frac{E_3 - E_3(T, T_1, T_2)}{\tau_3(T, T_1, T_2)} + \\ + (1 - \frac{h\nu_3}{h\nu_5})\frac{E_5 - E_5(T, T_3)}{\tau_{53}(T, T_3)} + (1 - \frac{h\nu_1}{h\nu_5} - \frac{h\nu_2}{h\nu_5})\frac{E_5 - E_5(T, T_1, T_2)}{\tau_5(T, T_1, T_2)} + \\ + (1 - \frac{h\nu_4}{h\nu_5})\frac{E_5 - E_5(T, T_4)}{\tau_{54}(T, T_4)} \quad (6)$$

Where the total gas kinetic energy E_k per unit volume is:

$$E_k = \left(\frac{5}{2} n_{N_2} + \frac{5}{2} n_{CO} + \frac{3}{2} n_{H_e} + \frac{5}{2} f n_{CO_2} \right) kT \tag{7}$$

Where $n_{CO} = (1- f)\, n_{CO_2}$ is the number density of CO molecules per unit volume.
Taking into consideration stimulated emission, spontaneous emission, and losses in the cavity yields the equation that describes the time evolution of the cavity light intensity:

$$\frac{dI_{v_0}}{dt} = \frac{-I_{v_0}}{\tau_c} + chv_0 \left(\frac{\Delta N W I_{v_0}}{h} + n_{001} P(J) S \right) \tag{8}$$

Where c is the light velocity, h is Planck constant, τ_c is photon life time in the cavity:

$$\tau_c = -\frac{2L}{c\left(\ln R_1 + 2\ln R_2\right)} \tag{9}$$

Where R_1 is the reflection coefficient of rear mirror, R_2 is the reflection coefficient of the output mirror, L is the resonator length. The expressions of W, S in the equation of (8) are:

$$W = \frac{\lambda^2 F}{4\pi^2 v_0 \Delta v_L \tau_{sp}} \tag{10}$$

$$S = \frac{2\lambda^2 \Delta v_N}{\pi A \tau_{sp} \Delta v_L} \tag{11}$$

Where λ is the laser wavelength, υ_0 is the laser frequency, $\Delta\upsilon_L$ is the laser transition line width, $\Delta\upsilon_N$ is the laser natural line width, τ_{sp} is the spontaneous emission rate, A is the cross section of the laser beam, $F=l/L$ is the filling factor, l is the length of gain media.
When the Q-switch is closed, the loss in the cavity is so high that there is no laser output and the laser intensity in the cavity is nearly zero. So the Eqs. (1)-(5) equal zero. In the five equations mentioned above, E_1 (the energy per unit volume stored in the CO_2 symmetrical stretching mode), E_2 (the energy per unit volume stored in the CO_2 bending mode), E_3 (the energy per unit volume stored in the CO_2 asymmetrical modes), E_4 (the energy per unit volume stored in the N_2 molecules), E_5 (the energy per unit volume stored in the CO molecules) are defined respectively by T_1, T_2, T_3, T_4, T_5. A computer program processed in MATLAB is used to solve the five nonlinear equations. The five temperatures and an estimated ambient temperature are the initial values of the laser after the Q-switch is opened.
After the Q-switch is opened, the transmittance of output mirror is t. Therefore the population number of upper levels falls sharp; the laser oscillates rapidly in a short time, and then engenders a giant pulse output. The mathematical model of Q-switched CO_2 laser consists of seven differential expressions, which are dE_1/dt, dE_2/dt, dE_3/dt, dE_4/dt, dE_5/dt, dE_k/dt, $dI\upsilon_0/dt$ respectively. The variables in these expressions are T_1, T_2, T_3, T_4, T_5, T, $I\upsilon_0$.There is six temperature variables in the differential expressions, therefore it is called six-temperature model.

The specific expressions of the seven coupled differential equations are represented by Eqs. (1)- (6) and (8). Based on the Runge–Kutta theory, the seven variables (T_1, T_2, T_3, T_4, T_5, T, and Iv_0) can be obtained through solving the differential equations. The laser output power can be obtained from Iv_0:

$$P_{out} = -\frac{A}{2}\ln(R_2) \times \frac{1 - R_2 - \alpha}{1 - R_2} \times I(t) \times 10^{-7} \quad (12)$$

Where a is the loss coefficient of output mirror.

3.2 The numerical calculation

3.2.1 The parameters of CO_2 laser

The experimental schematic diagram is shown in Fig. 2. The key parameters of laser just as follows: the inner diameter is 8 mm, the gain area length of discharge tube is 800mm and the mixed gas pressure is 3.3kPa. The gas ratio is Xe: CO_2: N_2: He=1:2.5:2.5:17.5. The radius of curvature of rear mirror is 3m and its reflectivity is 98.5%. The length of optical cavity resonator is 1200mm. The medium of acousto-optically modulator used in our experiment is Ge single crystal whose single pass transmittance is 90% for the wavelength 10.6μm. The first order diffraction efficiency of acousto-optically medium for linearly polarized light is about 80% in horizontal direction and optical aperture is 6×10 mm². The transmittance of output mirror is 39%.

3.2.2 The numerical calculation of six temperature model

The initial values of Q-switched CO_2 laser have been considered before the Q-switch is opened. Based on the measured results of the laser and related values of the equation parameters which are shown in table 1, the six-temperature model is used for simulating the process of dynamical emission in the acousto-optically Q-switched CO_2 laser. A computer program processed in MATLAB is used to solve the differential equations based on the Runge–Kutta theory. Considering the open time of acousto-optically Q-switch, the establishing time of laser pulse should be added the corrected value 0.85μs (Xie et al., 2010). Under those conditions, the variation of output power with time is shown in Fig. 4(a). At the same conditions, the calculation of rate equations is shown in Fig. 4(b).

Parameter	Numerical value	Parameter	Numerical value
v_1/c [1]	1337 cm^{-1}	h	6.626×10^{-27} erg·s
v_2/c [1]	667 cm^{-1}	B_{CO_2} [2]	0.4cm^{-1}
v_3/c [1]	2349 cm^{-1}	τ_{sp} [2]	0.2s
v_4/c [3]	2330 cm^{-1}	λ	10.6μm
v_5/c [3]	2150 cm^{-1}	c	2.998×10^{10}cm·s^{-1}
X_1 [2]	$5\times10^{-9}cm^3\cdot s^{-1}$	M_{CO_2} [3]	7.3×10^{-23}g
X_2 [2]	$3\times10^{-9}cm^3\cdot s^{-1}$	M_{CO} [3]	4.6×10^{-23}g
X_3 [2]	$8\times10^{-9}cm^3\cdot s^{-1}$	M_{N_2} [3]	4.6×10^{-23}g
X_4 [2]	$2.3\times10^{-8}cm^3\cdot s^{-1}$	M_{He} [3]	6.7×10^{-24}g
X_5 [2]	$3\times10^{-8}cm^3\cdot s^{-1}$	k	1.38×10^{-16}erg·K^{-1}

Table 1. Parameters used in the calculations 1 See reference (Rossmann et al., 1956), 2 See reference (Soukieh et al., 1998), 3 See reference (Smith & Thomson, 1978)

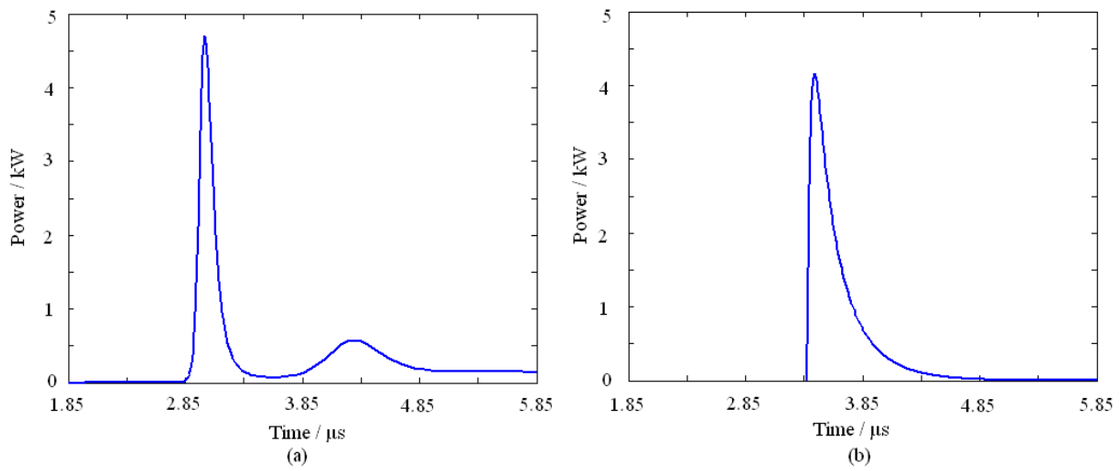

Fig. 4. Theoretical shapes of the pulsed laser (a) Calculated by six temperature model (b) Calculated by rate equations

3.2.3 Experimental device

The diagram of experimental device is shown in Fig.4. The path of laser output will be changed by the mirror first, and then the laser is divided into two paths by a beam splitter (a coated ZnSe mirror whose transmittance is 30%). One path of laser is accepted by the detector, and then the laser pulse waveform will be displayed by the oscilloscope after enlarged by the amplifier. The other path of laser is monitored by the power meter at the same time.

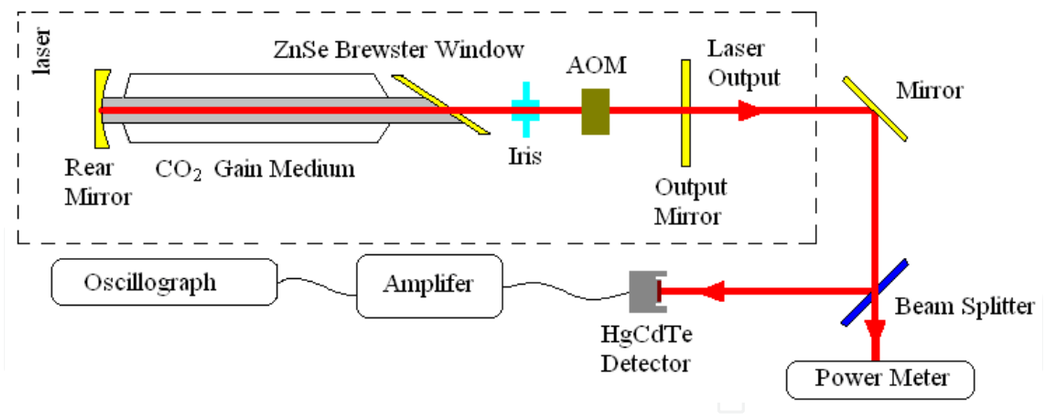

Fig. 5. Diagram of experimental device

When the transmittance of output mirror is 39% and the repetitive frequency is 5 kHz, the Q-switched pulsed laser is detected by a photovoltaic HgCdTe detector with the model of PV-10.6 made by VIGO Company, and the laser waveform is monitored on a TDS3052B digital storage oscilloscope with 500-MHz bandwidth. The shapes of the pulsed laser are shown in Fig.6, with a 160 ns pulse width and a 3μs delay time. The average power is 1.14 W which is measured by the power meter with the model of LP-3C made by Bejing WuKe Photo Electricity Company. Thus the average output power of this device is 3.8 W (light splitting ratio is 3:7), and the peak power of this laser is 4750 W.

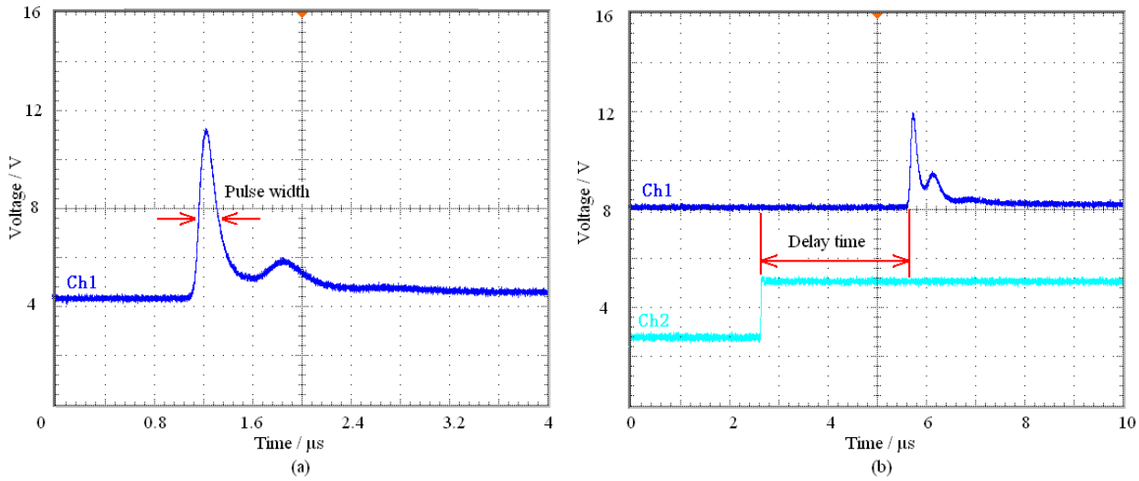

Fig. 6. Measurement shapes of the pulsed laser: (a) pulse width, (b) delay time. (Ch1 is Laser pulse waveform; Ch2 is transistor-transistor logic trigger signal)

A conclusion can be drawn by comparing figure 4 with figure 6. The measured results of peak power, pulse width and establishing time of laser pulse are in agreement with the theoretical calculations by rate equations as well as six-temperature model. The tail phenomenon is obvious in the calculation by six-temperature model, which is more consistent with the experimental result. The six-temperature model more perfectly explains the behavior of energy transfer between different molecules in the laser gain medium, and analyzes the influence of gas temperature on laser output. However the rate equations can only explain the particle population transfer between up and down energy levels. Therefore the six-temperature model gives a more correct analysis than the rate equations. The comparison of theoretical calculations and experimental results are shown in table 2.

Comparing results	rate equations	six temperature model	experimental result
Pulse width/ns	200	166	160
Peak power/kW	4.15	4.7	4.75
Pulse delay time/μs	3.35	2.9	3
Tail phenomenon	Not obvious	Obvious	Obvious

Table 2. The comparison of theoretical calculations and experimental results

4. The optimum design of acousto-optically Q-switched CO_2 laser

Some parameters (The optical loss in cavity, the transmittance of output mirror, etc) of laser have great influence on laser output. When an acousto-optically Q-switched CO_2 laser is to be designed, those factors must be considered. In the following section, the further theoretical calculations and experimental methods will be introduced to guide the optimum design of laser.

4.1 The influence of acousto-optically Q-switch on laser output

The medium of acousto-optically modulator used in our previous experiments is Ge single crystal whose single pass transmittance is 90% for the wavelength 10.6μm. The influence of absorption coefficient of acousto-optically crystal on laser output has been described in

detail (Xie et al., 2010). And the high absorption coefficient is one of the most important factors to hinder the development of acousto-optically Q-switched CO_2 laser. In order to further clarify the influence degrees of the absorption coefficient on laser output, the variation of output power with single pass transmittance(δ) has been simulated by six-temperature model when other parameters of laser are invariable just as Fig.7. The calculations show that when the acousto-optically modulator has higher single pass transmittance, the peak power of pulse laser will be higher, and the establishing time of laser pulse will be shorter. When the single pass transmittance is increased by 2 percent, the increment of peak power of pulse laser is about 6 percent. With the development of crystal process technology, the crystal with higher single pass transmittance would be manufactured (The maximum value of best acousto-optically crystal is higher than 94% presently), and then the performance of acousto-optically Q-switched CO_2 laser output would be further enhanced.

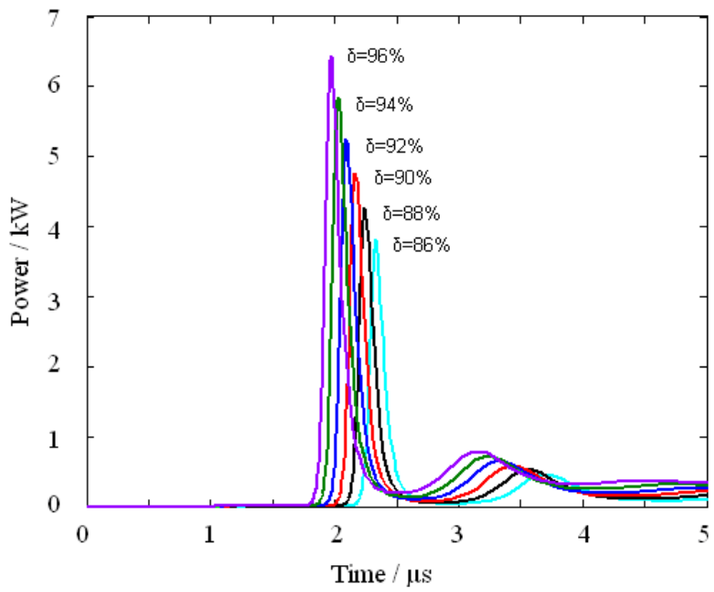

Fig. 7. Output power of the laser versus time at different single pass transmittance

4.2 The influence of output mirror transmittance on laser output

When the transmittance (*t*) of output mirror is 18%, 25%, 32%, 39%, 46%, and 53% separately, a computer program processed in MATLAB is used to solve the differential equations based on the Runge–Kutta theory. Figure 8 shows the variation of light intensity in the cavity with time. The light intensity is reduced with increasing of the transmittance gradually. And when the increment of the transmittance is 7 percent, the decrease in light intensity is almost 28 percent. Then the laser pulse waveform is calculated by Eq. (12) at different transmittances as in figure 9, which shows that the influence of transmittance on output power is obvious. The peak power is a function of output mirror transmittance when other conditions remain unchanged (just as shown in imaginable line in figure 9). The theoretical results show that the peak power has a maximum when it changes with transmittance, which lays a theoretical foundation for the optimization of laser parameter.

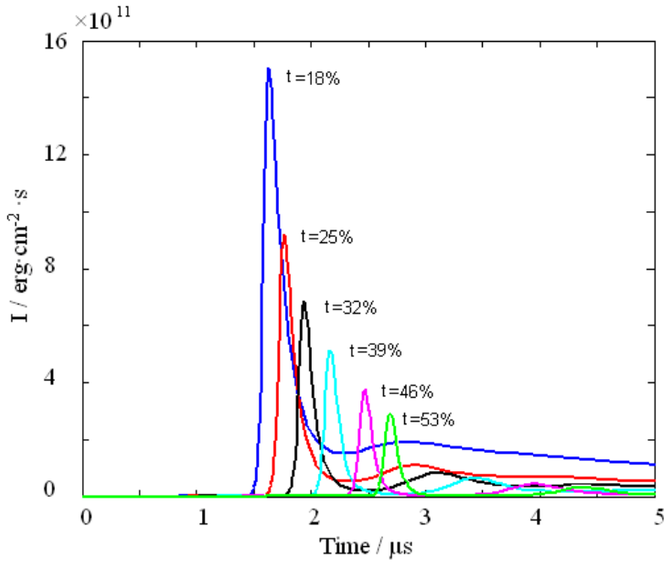

Fig. 8. Light intensity in the laser cavity versus time at different transmittance

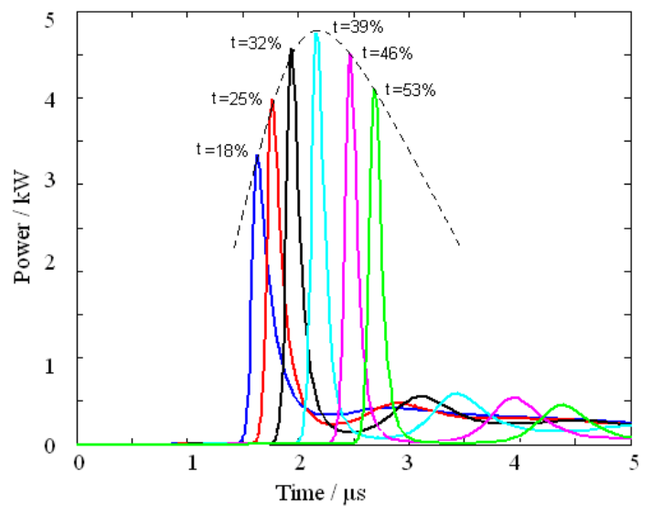

Fig. 9. Output power of the laser versus time at different transmittance

According to the simulation results above, our laboratory has manufactured a group of ZnSe output mirrors (the transmittances are 18%, 25%, 32%, 39%, 46%, 53% separately, and the aperture size all are 30mm). Performance characteristics have been investigated as a function of output mirror transmittance with an acousto-optically Q-switch. At 5 kHz pulse repetition frequency, the average power and pulse width are measured for each mirror independently, and then the peak power of laser is calculated. The quadratic fitting curves of peak power and pulse width versus the transmittance of output mirror are shown in Fig.10. Compared with imaginable line in Fig.9, the experimental results agree well with that of the six-temperature model theory. The transmittance of output mirror has a significant influence on the peak power and pulse width of acousto-optically Q-switched CO_2 laser, and the optimal value of transmittance is 39% in the experiment.

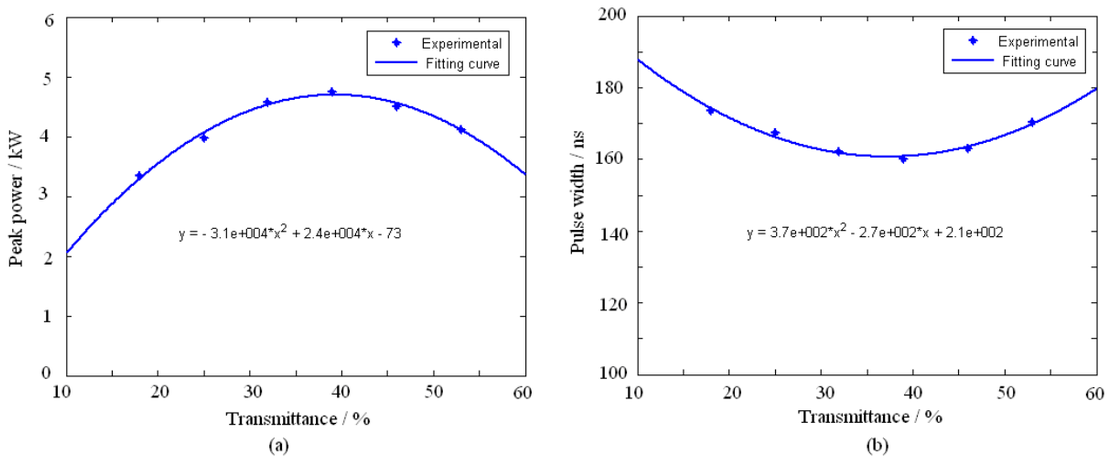

Fig. 10. The fitting curves of peak power (a) and the pulse width (b) versus transmittance of the output mirror

4.3 The influence of iris on output laser

Higher requirement of laser quality has been tendered in the fields of scientific research and engineering applications. In order to meet this demand, an iris is inserted in the resonator to obtain laser with basic mode. The influence of aperture size of iris on laser output is investigated when the transmission of output mirror is 39%. The fitting curves of peak power and pulse width versus the pulse repetition frequency are shown in Fig.11 individually at different aperture size. Just as Fig.11 shows, at the same pulse repetition frequency, when the size of aperture is decreased, the peak power is reducing and the pulse width is increasing. That is because the marginal laser oscillation is limited by the iris, the mode volume of laser cavity is reduced. Therefore, the better quality of laser, the lower peak power will be obtained.

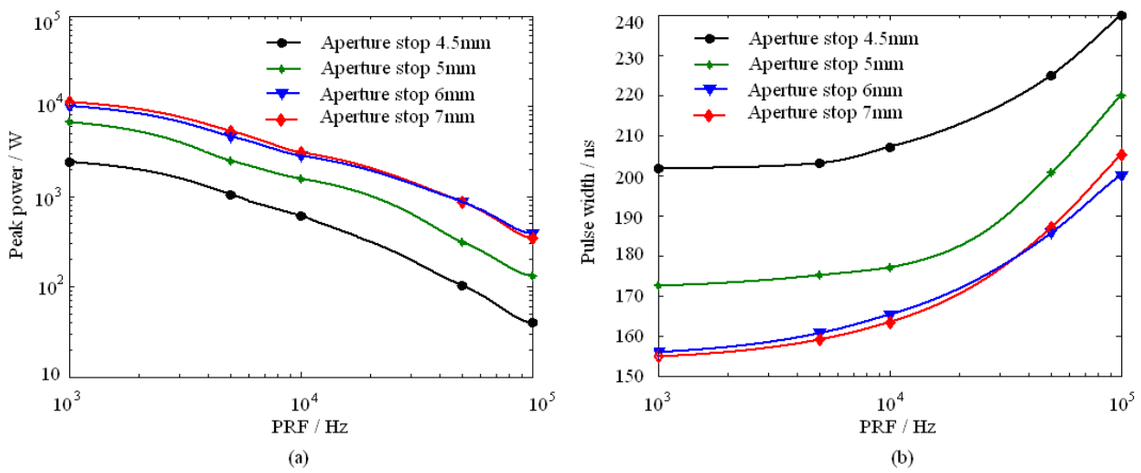

Fig. 11. Peak power (a), pulse width (b) of the CO_2 laser as a function of apertures stop

There are many vibrational-rotational levels in CO_2 molecules. The calculated results show that the total energy available for extraction is the energy stored in all the rotational levels for the case of long weak pulse, whereas for the case of very short pulses only the energy stored in the active rotational sublevel is available (Smith & Thomson, 1978). When the aperture size of iris is small, the iris will limit oscillation of marginal laser. Under this condition, more rotational levels are needed to participate in excited emission so as to realize laser output, therefore the pulse width of laser is wide and the peak power is low. The pulse width is reduced gradually with the increasing of aperture size. When the aperture size is over 6 mm, the pulse width will increase with the increasing of aperture size at high repetition frequency (pulse repetition frequency ≥ 40 kHz). That is to say, when the aperture size is over 6 mm, the iris just limits laser oscillations between some weaker levels. Under this condition, a bigger gain volume is obtained, at the same time, the pulse width is effectively compressed and the quality of laser is improved. The optimal aperture size of iris is 6mm in our experiment. The laser mode is shown in Fig.12.

Fig. 12. Laser mode

4.4 Output performance of pulse repetition frequency

According to theoretical and experimental research mentioned above, the performance of laser output is better when the transmittance of output mirror is 39% and the aperture size of iris is 6mm. The discharge current is from 8mA to 16mA, and maximum output power is 22 W. When inserting the acousto-optically modulator, the maximum output power is decreasing to 9.5 W. The laser output mode is TEM_{00}. The pulsed frequency range is from 1 Hz to 100 kHz. The pulsed waveforms of 10.6μm with repetition rate 1 kHz measured by HgCdTe detector (VIGO PC-10.6) are shown as Fig.13. The output pulsed width is about 156 ns as shown in Fig. 13(a) (channel 1) and channel 2 is transistor-transistor logic trigger signal. The pulsed establishing time is 2.9μs, at that time the measured average power is 1.56 W. The output stability of laser is quite well in high repetition frequency, which the pulsed amplitude difference is smaller than ±5% as shown in Fig. 13(b).

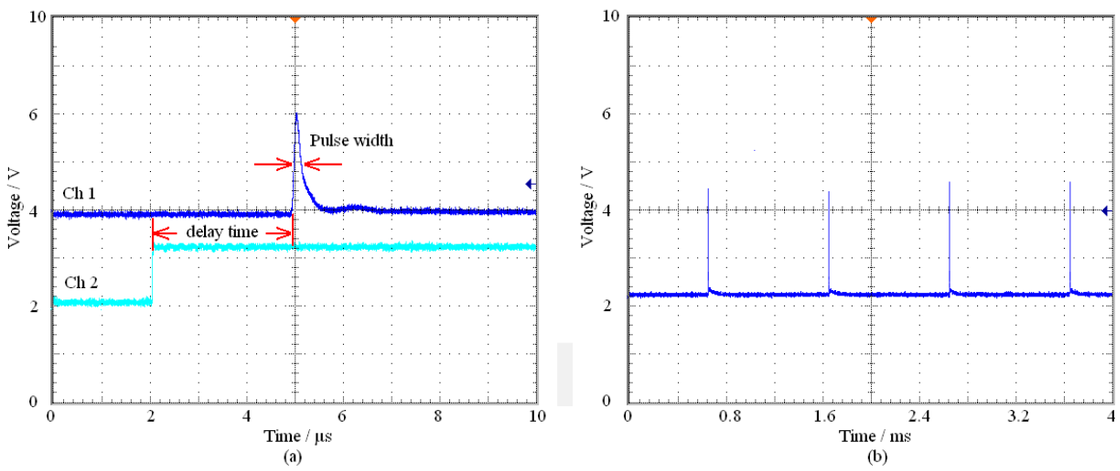

Fig. 13. Output waveforms of CO_2 laser at 1 kHz

5. Tunable acousto-optically Q-switched CO_2 laser

The CO_2 laser has more than 100 spectral lines between 9-11μm, among which several spectral lines next to 10.6μm have the maximum gain (Qu et al., 2005; Ma et al., 2002). Therefore the output spectral line for non-tunable CO_2 laser is 10.6μm. Through the technology of wavelength tuning, the spectral lines between 9-11μm would be obtained one by one. The technologies of wavelength tuning for pulse CO_2 laser include injection locking (Menzise et al., 1984), Fabry-Perot (F-P) etalon (Wu et al., 2003), and grating tuning (Izatt et al, 1991). The injection locking often can not obtain single line output, and it needs complicated techniques, so this method is not suitable for compacted CO_2 laser in engineering applications. Although tuning with F-P etalon has the advantage of simple structure and easy operation, but it only applies to the case when the gain length of laser is shorter, so it can not obtain high power laser output. The diffracting character of grating determines that it has a good capability of wavelength tuning. By changing the incident angle on the grating, the laser output wavelength can be selected. Therefore we designed tunable acousto-optically Q-switched CO_2 laser using the grating as a tuning device.

5.1 The principle of grating tuning

The relationship between diffraction angle, grating constant and wavelength can be obtained by the grating equation just as follows.

$$d(\sin\alpha + \sin\beta)=m\lambda \tag{13}$$

Where d is the grating constant, α is the incident angle of laser, β is the diffraction angle of laser, m is the order of diffraction, λ is the laser wavelength. The resonator is composed by rear mirror (or lens) and grating, and it usually works under the condition of Littrow autocollimator (Wang, 2007). That is to say, the direction of first order diffraction of grating is in consistent with optical axis. At that time, the incident angle α equals diffraction angleβ, and the grating equation (13) will be replaced by equation (14).

$$2d\sin\alpha=m\lambda \tag{14}$$

Equation (14) shows that under the Littrow autocollimator condition, the spectral lines which satisfy the grating equation could sustain oscillation in the resonator, and the other spectral lines could not sustain oscillation because of the bigger diffracting loss. Incident angle (α) is determined by the grating constant (*d*). And the diffraction efficiency or the light distribution of each order is depends on the shape of grating grooves, the character of grating incidence surface, the polarized character of incident light, etc. (Bayin et al, 2004). An effective method to improve diffraction efficiency of single-order is to reduce the diffraction series. Through limiting the grating constant (*d*), the diffraction angles of other diffraction orders except the first order would go beyond the grating reflective surface, so its corresponding diffracted light do not exist in fact. To meet that condition, the grating constant that is corresponding with the selected laser wavelength should satisfy the relationship just as follows.

$$0.5\lambda < d < 1.5\lambda \tag{15}$$

Thus, the grating constant (*d*) corresponding with wavelength tuning range of CO_2 laser (9μm-11μm) would be 5.5μm- 13.5μm and the value of grating groove is 74 - 181 lines /mm.

5.2 The device of grating tuning

The output mirror is replaced by grating to realize the wavelength tuning of acousto-optically Q-switched CO_2 laser. Based on the principles of grating tuning, laser wavelength tuning device is designed just as Fig.14. The grating and mirror1 which are placed on the horizontal rotary table must be vertical to the surface of the rotary table and ensure that their intersection coincides with the axis of rotary table. The direction of diffraction grating is horizontal, and the angle between grating and mirror1 is 60°. At this time, the angle between the laser output reflected by mirror1 and the optical axis of laser is 60° too. Then the output laser will be changed direction by the mirror2 to obtain a reasonable direction. The working way of grating is first order oscillation and zero order output. According to the results of theoretical and experimental analysis, the metal engraved grating (120lines/mm) is manufactured with blaze wavelength of 10.6μm and its first order diffraction efficiency is about 60%.

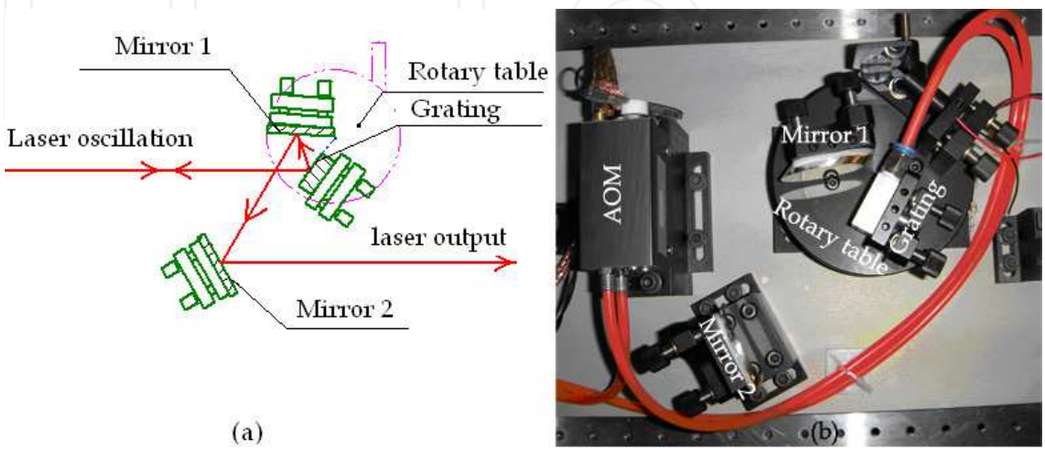

Fig. 14. Device of grating tuning. (a) The schematic, (b) The Photoshop

5.3 Output performance of grating tuning

The spectrum lines are measured by the spectrum analyzer under the working condition of Q-switch, just as shown in figure 15. There are 67 lines which average power of single line is over 2.5W among 9.18μm -10.88μm, and the highest average power is about 8 W. According to the measured spectrum distribution, the spectrum lines of 10R/10P are abundant, and the average power is higher compared with the spectrum lines of 9R/9P. The output power of laser greatly different in different wave bands since the different laser gains in different wavelength and the grating diffraction efficiency variation.

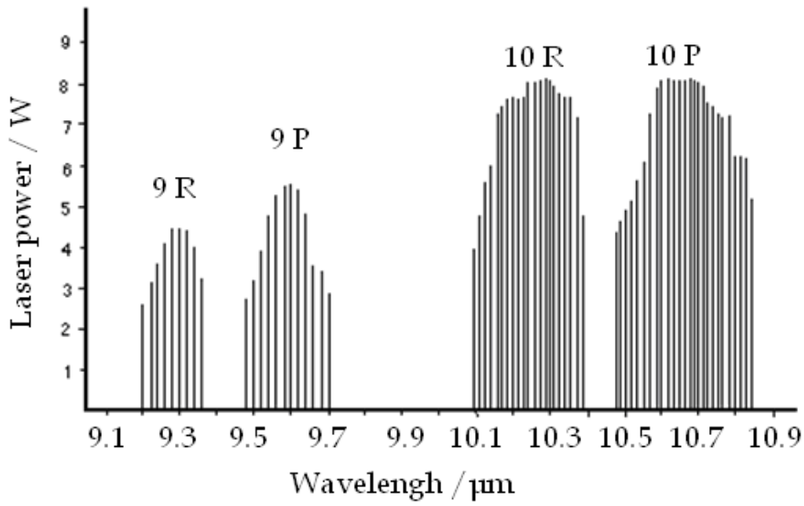

Fig. 15. Laser Spectral Lines

6. The application of acousto-optically Q-switched CO_2 laser

One of the outstanding CO_2 laser features making it suitable for optoelectronic countermeasure applications relates to its distinctive emission spectrum composed of several tens of particular output lines situated in the 9-11μm wavelength range (Atmospheric window)(Yin & Long, 1968). And the laser jamming is a priority research area of optoelectronic countermeasure (LIQIN et al., 2002; Wang et al., 2010). Thresholds for laser jamming in detectors depend on jamming mechanisms, irradiation time, beam diameter, detector dimensions, optical and thermal properties of the materials used in detector construction, quality of thermal coupling to the heat sink, etc. (Bartoli et al., 1976; Evangelos et al., 2004; Sun et al., 2002). The optoelectronic detector (high sensitivity, high signal-to-noise ratio) is irradiated by CO_2 laser, which would induce the saturation effect and lead to signal loss of detector (Bartoli et al., 1975). Since these parameters can vary considerably from one detector to another, it would be very costly and impractical to measure damage thresholds for every case of interest.

A compacted multifunctional acousto-optically Q-switched CO_2 laser is constructed just as shown in Fig.16. The range of repetition frequency could adjust from 1 Hz to 100 kHz, and the tuning range of output wavelength is from 9.2μm to 10.8μm. The spot diameter is 5 mm and the laser mode is basic mode.

Fig. 16. Tunable acousto-optically Q-switch CO_2 laser

6.1 Experimental device of laser irradiate detector

Fig.17 shows the schematic diagram of detector irradiated by pulse laser. HgCdTe detectors with the model of PV-10.6 and PC-10.6 made by VIGO Company are researched in our experiments separately. The spot diameter would be limited at 5 mm by the iris. The power density reaching to the photo-sensitive surface of detector is continuously adjustable through adjusting the attenuators inserted in the light path. The beam splitter is a coated ZnSe plat mirror whose transmittance is 30%. The optical components need to be adjusted to make the laser pass the geometric center of every component.

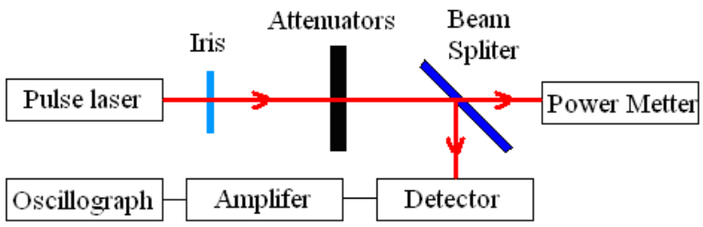

Fig. 17. Experimental schematic of detector irradiated by pulse laser

6.2 The experiment of laser jamming

During laser irradiation, the incident laser power density could increase continuously. The criterion of interference and saturation phenomenon for HgCdTe detector is as follows: when the top of output voltage waveform of detector emerge distorted phenomenon, the detector has been subjected to disturbance; when the peak value of output voltage keeps invariant as the incident laser power grows, the detector is saturated. The average power of the laser is measured by power meter and it is changed into the average power at the photo-sensitive surface of detector, and then the power density could be obtained.

6.2.1 The experiment of laser jamming for PC-10.6 detector

Before Irradiation, the transmittance of attenuators should be adjusted to minimum so as to protect the detector. The detector is irradiated by pulse laser with pulse repetition frequency of 1 kHz. The duration of laser irradiation on detector is 0.5s each time, and then the output voltage waveform of detector would be recorded by the oscilloscope after each irradiation. The detector would be continuously irradiated by pulse laser after it return to nature. The voltage waveform of detector is shown in figure 18(a) when it works at normal condition. The output voltage waveform is monitored as the attenuation is decreased continuously so

as to judge the interference phenomenon. The laser power density of photo-sensitive surface is the disturbance threshold as soon as the detector is been disturbed. At this time, the output voltage waveform is shown just as figure 18(b), and the disturbance threshold is 0.452W/cm². Then decrease the attenuation continuously and observe the output voltage waveform to judge the saturation phenomenon. The laser power density of photo-sensitive surface is the saturation threshold as soon as the detector is saturated. At this time, the output voltage waveform is shown just as figure 18(c), and the saturation threshold is 1.232W/cm². Henceforth, the output voltage amplitude of the detector could not increase obviously with the increasing of laser power density. The output voltage waveform is shown just as figure 18(d), and the detector is saturated completely. At this time, the laser power density that reaches to the photo-sensitive surface of detector is 12.883 W/cm². Pause a moment, the detector will restore again, therefore the detector has not been damaged.

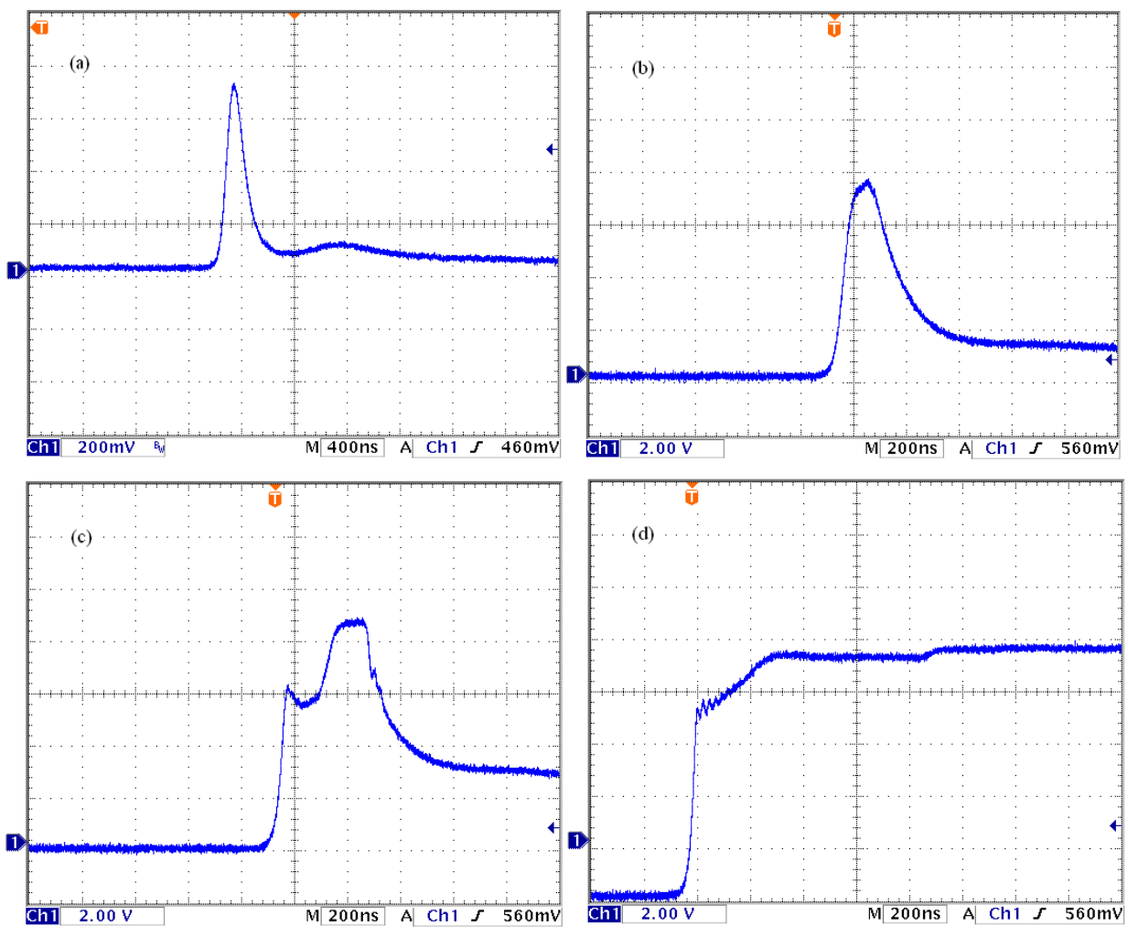

Fig. 18. Experimental results of PC-10.6 detector irradiated by pulse laser: (a) Normal working, (b) Disturbance phenomenon, (c) Saturation phenomenon, (d) Saturation completely

The response curve of PC-10.6 detector irradiated by pulse laser is shown in Fig.19. The output voltage amplitude increases linearly with the increase of power density, and when the power density increases to a certain value (saturation threshold), the output voltage amplitude will drive to plateau. At this time, the detector is saturated.

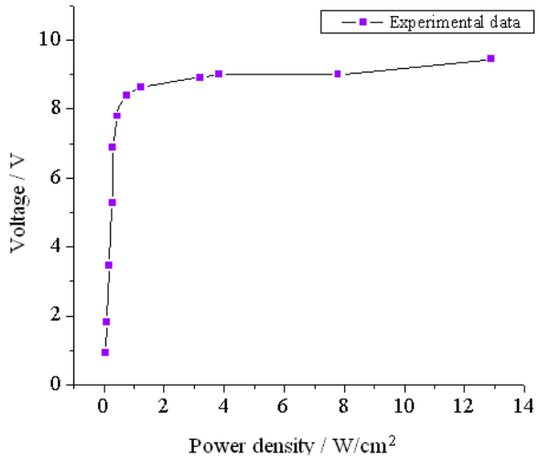

Fig. 19. The response curve of PC-10.6 detector irradiated by pulse laser

6.2.2 The experiment of laser jamming for PV-10.6 detector

The jamming experiments on PV-10.6 detector have been done by using the same method with that of PC-10.6 detector. The measured results are as follows: the disturbance threshold is 0.452W/cm², the saturation threshold is 0.345 W/cm², and the power density of complete saturation is 2.820 W/cm². The output voltage waveforms of detector are shown in figure 20.

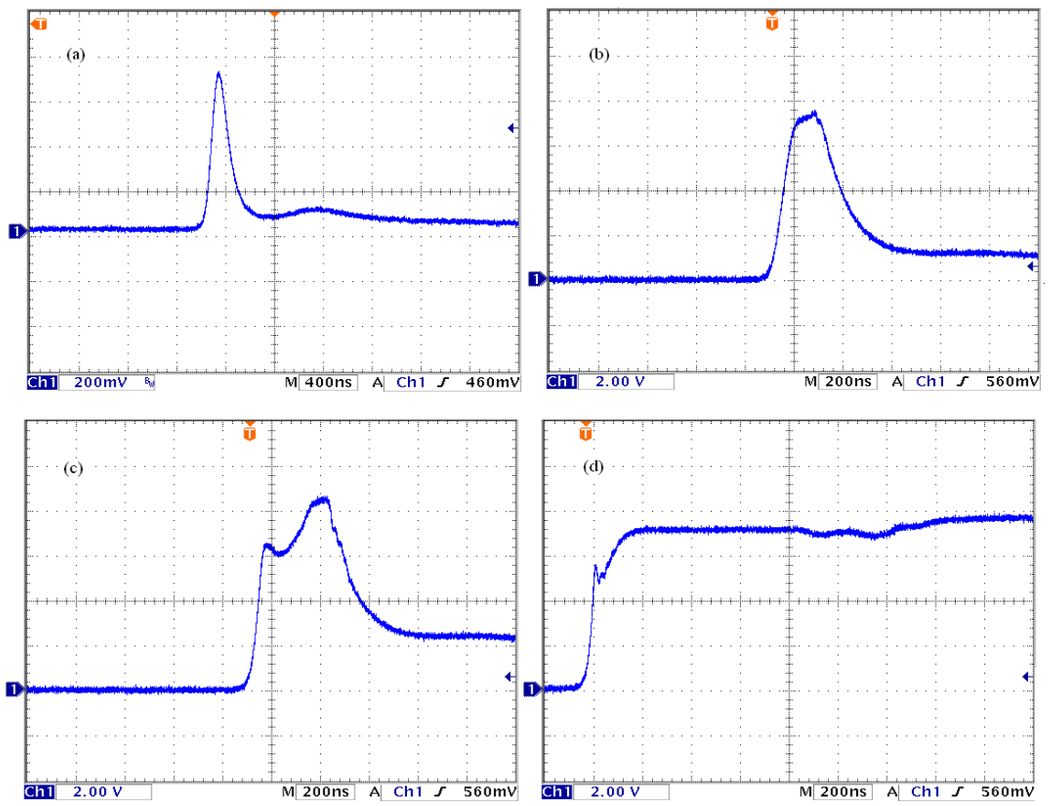

Fig. 20. The experimental results of PV-10.6 detector irradiated by pulse laser: (a) Normal working, (b) Disturbance phenomenon, (c) Saturation phenomenon, (d) Saturation completely

The response curve of PV-10.6 detector irradiated by pulse laser is shown in Fig.21. Its variable tendency is similar to the PC-10.6 detector, but its disturbance threshold and saturation threshold are lower than the PC-10.6 detector. The PV-10.6 detector is prone to be disturbed by the pulse laser.

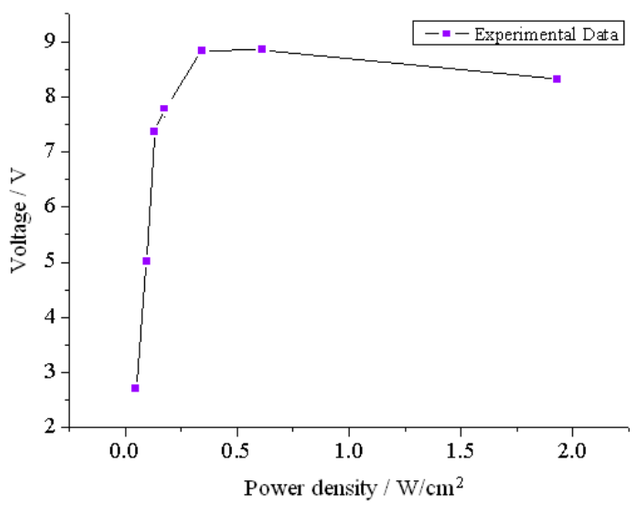

Fig. 21. The response curve of PV-10.6 detector irradiated by pulse laser

6.3 The influence of pulse repetition frequency on the threshold of detector

The pulse repetition frequency of CO_2 laser has great influence on disturbance threshold and saturation threshold of detector. Based on the experimental method mentioned above, the PC-10.6 HgCdTe detector is irradiated by pulse laser with pulse repetition frequency at 1 kHz, 5 kHz, 10 kHz, 20 kHz, 30 kHz, 40 kHz, and 50 kHz respectively. Then the disturbance threshold and saturation threshold of detector are obtained at different pulse repetition frequency. The variations of detector threshold with pulse repetition frequency are shown in Fig.22. Both the disturbance threshold and saturation threshold are reduced with the increase of pulse repetition frequency, and the decline of threshold is even faster at high frequency. When the detector is working at normal condition, the current carriers of heat balance would keep unchanged, and the resistance of detector depends on the photo-generated carriers only. Laser irradiation with multi-pulse is a course of thermal accumulation. When the detector is irradiated by multi-pulse laser, it could not be cooled quickly in one pulse period so that the temperature of detector will arise. At that time, the powerful pulse laser not only engenders the photo-generated carriers, but also engenders current carriers of heat balance. The current carriers of heat balance will lead to the higher dark resistance which would disturb the normal working of detector. The higher the frequency, the more obvious the thermal accumulation, and the detector would be disturbed more easily. Therefore the development of laser with high pulse repetition frequency used in the field of laser irradiation has great scientific significance.

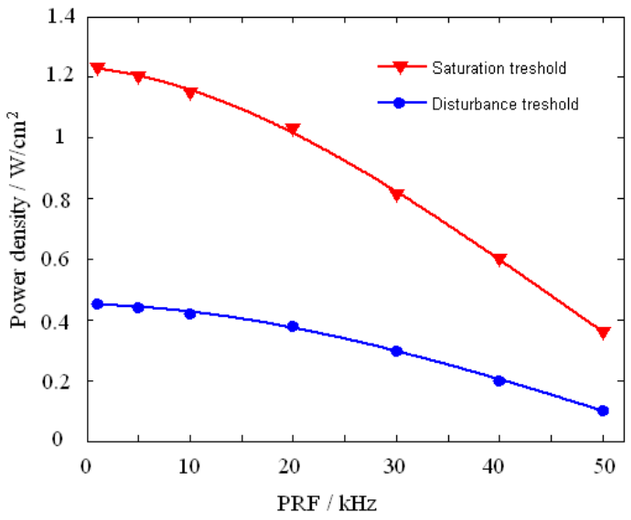

Fig. 22. Variations of detector threshold with pulse repetition frequency

7. References

Bartoli, F. J.; Esterowitz, L.; Kruer, M. R. & Allen, R. E. (1975). Thermal recover processes in laser irradiated HgCdTe (PC) detectors. *Applied Optics*. Vol.14, No. 10, (May 1975), PP. 2499-2507, ISSN 0003-6935

Bartoli, F.; Esterowitz, L.; Allen, R. & Kruer, M. (1976). A generalized thermal modal for laser damage in infrared detectors. *Journal of Applied Physics*. Vol. 47, No.7, (June 1975), PP. 2875-2881, ISSN 0021-8979

Bayanheshig; Gao, J. X.; Qi, X. D. & Li, C. Q. (2004). Manufacture for High Diffraction Efficiency Grating in the First-order Output of 10.6μm Laser. *Journal of Optoelectronics Laser*. Vol. 15, No.10, (January 2004) PP.1137-1140, ISSN 1005-0086, (In Chinese)

Carr, L.; Fletcher, L. ; Crittenden, M.; Carlisle, C. ; Gotoff, S. ; Reyes, F. & Francis, D. (1994). Frequency-agile CO_2 DIAL for environmental monitoring. *SPIE*, Vol.2112, PP.282-294, ISBN 9780819414038, Atlanta, USA

Chang, L. & Jiang, Y. (2009). Effect of Laser Irradiation on $La_{0.67}Ba_{0.33}MnO_3$ Thin Films. *Acta Physica Sinica*.Vol.58, No.3, (July 2008), PP. 1997-2001. ISSN 1000-3290 (In Chinese)

Evangelos, T. Juntaro, I. & Nigel, P. (2004). Absolute linearity measurements on HgCdTe detectors in the infrared region. *Applied Optics*.Vol.43, No.21, (January 2004), PP.4182-4188, ISSN 0003-6935

Hedayatollahnajafi, S.; Staninec, M.; Watanable, L.; Lee, C. & Fried, D. (2009). Dentin bond strength after ablation using a CO_2 laseroperating at high pulse repetition rates. *SPIE*. Vol.7162, PP.71620F0-9, ISBN 9780819474087, San Jose, USA

Hong, L.; Li, L. & Ju, C. (2002). Investigation of cutting of engineering ceramics with Q-switched pulse CO_2 laser. *Opticsand Lasers in Engineering*. Vol.38, (June 2001), PP. 279-289, ISSN 0143-8166

Izatt, J. R.; Rob, M. A. &Zhu. W. S. (1991). Two-and three-grating resonators for high-power pulsed CO_2 lasers. *Applied Optics*. Vol. 30, No. 30, (January 1990), PP.4319-4329, ISSN 0003-6935

Kariminezhad, H.; Parvin, P.; Borna, F. &Bavali, A. (2010). SF_6 leak detection of high-voltage installations using TEA-CO_2 laser-based DIAL. *Optics and Lasers in Engineering*. Vol.48, (May 2009), PP. 491-499, ISSN 0143-8166

Kovacs, M. A.; Flynn,C. & Javan, W. A. (1966) . Q witching of molecular laser transitions. *Applied Physics Letter.* Vol. 8, No. 3, (December 1965), PP. 61-62, ISSN 0003-6951

LIQIN, M.; XIANGAI, X.; XIAOJUN, X.; WENYU, L. & QISHENS, L. (2002). Chaos in photovoltaic HgCdTe detectors under laser irradiation. *Applied physics B.* Vol75, (April 2002), PP.667-670, ISSN 0946-2171

Ma, Y. & liang, D. (2002). Tunable and frequency-stabilized CO_2 waveguide laser. *Optical Engineering*. Vol.41, No.12, (February 2002), PP. 3319-3323, ISSN 0091-3286

Manes, K. R. & Seguin, H. J. (1972). Analysis of the CO_2 TEA laser. *Journal of Apply Physics*. Vol.43, No.12, (March 1972) PP.5073-5078, ISSN 0021-8879

Menzise, R. T.; Flamant, P. H.; Kavaya, M. J. & Kuiper, E.V. (1984). Tunable mode and line selection by injection in a TEA CO_2 laser. *Applied Optics.*Vol.23, No.21, (May 1984), PP.3854-3861, ISSN 0003-6935

Qu, Y.; Ren, D.; Hu, X.; Liu, F.; Zhang, L. & Chen, C. (2005). Wavelength measurement of tunable TEA CO_2 laser. *SPIE*. Vol. 5640, PP. 564-567, ISBN 9780819455956, Beijing, China

Rossmann, K.; France, W. L.; Rao, K. N. & Nielsen, H. H. (1956). Infrared Spectrum and Molecular Constants of Carbon Dioxide. *The Journal of Chemical Physics*. Vol. 24, No.5, (July 1955), PP.1007-1008, ISSN 0021-0606

Smith, K. & Thomson, R. M. (1978). *Computer Modeling of Gas Laser,* Plenum Press, ISBN 0-306-31099-6, New York

Soukieh, M.; Ghani, B. A. & Hammadi, M. (1998). Mathematical modeling of CO_2 TEA laser. *Optical & laser Technology*, Vol.30, (August 1998), PP. 451-457, ISSN 0030-3992

Sun, C. W.; Lu, Q. S.; Fan, Z. X.; Chen, Y. Z; Li, C. F.; Guan, J. L. & Guan, C. W. (2002). *Effects of laser irradiation.* National defense industry Press, ISBN 7-118-02451-0 Beijing, (In Chinese)

Tian, Z. S.; Wang, Q.; & Wang, C. H. (2001). Investigation of the pulsed heterodyne of an electro-optically Q-switched radio-frequency-excited CO_2 waveguide laser with two channels. *Applied Optics.*Vol.40, No.18, (June 2000), PP.3033-3037, ISSN 0003-6935

Wang, S. W.; LI, Y.; Guo, L. H. & Guo, R. H. (2010). Analysis on the disturbance of CO_2 laser to long-wave infrared HgCdTe detector. *J. infrared Millim. Waves*. Vol.29, No.2, (March 2009), PP.102-104, ISSN1001-9014 (In Chinese)

Wang, Z. J. (2007). *Practical Optics Technical Manual*. Machine Press, ISBN 9787111198178 Beijing, (In Chinese)

Wu, J.; Wan, C.; Tan, R.; Wang, D. & Tang Y. (2003). High repetition rate TEA CO_2 laser with randomly coded wavelength selection. *Chinese optics letters*. Vol. 1, No.10, (June 2003), PP.601-603, ISSN1671-7694

Xie, J. J.; Guo, R. H.; Li, D. J.; Zhang, C. S.; Yang, G. L. & Geng, Y. M. (2010). Theoretical calculation and experimental study of acousto-optically Q-switched CO_2 laser. *Optics Express*. Vol.18, No.12, (March 2010), PP.12371-12380, ISSN 0925-3467

Yin, P. K. L. & Long. P. K. (1968). Atmospheric Absorption at the Line Center of P (20) CO_2 Laser Radiation. *Applied optics*. Vol.7, No. 8, (February 1968), PP. 1551-1553, ISSN 0003-6935

Zelinger, Z.; Strrizik,; Kubat, M.; Civis, P.; Grigorova, E.; Janeckova, R.; Zavila, O.; Nevrly, V.; Herecova, L.; Bailleux, S.; HorKa, V.; Ferua, M.; Skrinsky, J.; kozubkova, M.; Drabkova, S. &Janour, Z. (2009). Dispersion of Light and Heavy Pollutants in Urban Scale Models: CO_2 Laser Photoacoustic Studies. *Applied Spectroscopy*. Vol.63, No.4, (August 2008), PP.430-436, ISSN 0003-7028

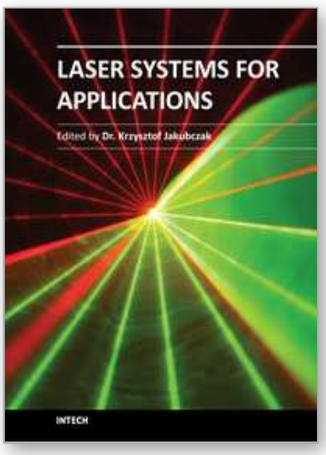

Laser Systems for Applications

Edited by Dr Krzysztof Jakubczak

ISBN 978-953-307-429-0
Hard cover, 308 pages
Publisher InTech
Published online 14, December, 2011
Published in print edition December, 2011

This book addresses topics related to various laser systems intended for the applications in science and various industries. Some of them are very recent achievements in laser physics (e.g. laser pulse cleaning), while others face their renaissance in industrial applications (e.g. CO2 lasers). This book has been divided into four different sections: (1) Laser and terahertz sources, (2) Laser beam manipulation, (3) Intense pulse propagation phenomena, and (4) Metrology. The book addresses such topics like: Q-switching, mode-locking, various laser systems, terahertz source driven by lasers, micro-lasers, fiber lasers, pulse and beam shaping techniques, pulse contrast metrology, and improvement techniques. This book is a great starting point for newcomers to laser physics.

InTech Europe
University Campus STeP Ri
Slavka Krautzeka 83/A
51000 Rijeka, Croatia
Phone: +385 (51) 770 447
Fax: +385 (51) 686 166
www.intechopen.com

InTech China
Unit 405, Office Block, Hotel Equatorial Shanghai
No.65, Yan An Road (West), Shanghai, 200040, China
中国上海市延安西路65号上海国际贵都大饭店办公楼405单元
Phone: +86-21-62489820
Fax: +86-21-62489821

IntechOpen